HHS Public Access

Author manuscript

Cell Rep. Author manuscript; available in PMC 2020 September 21.

Published in final edited form as:

Cell Rep. 2019 July 23; 28(4): 1103–1116.e4. doi:10.1016/j.celrep.2019.06.073.

Integrating Gene and Protein Expression Reveals Perturbed Functional Networks in Alzheimer's Disease

Saranya Canchi[1,2], **Balaji Raao**[1], **Deborah Masliah**[1], **Sara Brin Rosenthal**[3], **Roman Sasik**[3], **Kathleen M. Fisch**[3], **Philip L. De Jager**[4], **David A. Bennett**[5], **Robert A. Rissman**[1,2,6,*]

[1]Department of Neurosciences, University of California, San Diego, La Jolla, CA, USA

[2]Veterans Affairs San Diego Healthcare System, San Diego, CA, USA

[3]Center for Computational Biology & Bioinformatics, Department of Medicine, University of California, San Diego, La Jolla, CA, USA

[4]Center for Translational & Computational Neuroimmunology, Department of Neurology, Columbia University Medical Center, New York, NY, USA

[5]Rush Alzheimer's Disease Center, Rush University Medical Center, Chicago, IL, USA

[6]Lead Contact

SUMMARY

Asymptomatic and symptomatic Alzheimer's disease (AD) subjects may present with equivalent neuropathological burdens but have significantly different antemortem cognitive decline rates. Using the transcriptome as a proxy for functional state, we selected 414 expression profiles of symptomatic AD subjects and age-matched non-demented controls from a community-based neuropathological study. By combining brain tissue-specific protein interactomes with gene networks, we identified functionally distinct composite clusters of genes that reveal extensive changes in expression levels in AD. Global expression for clusters broadly corresponding to synaptic transmission, metabolism, cell cycle, survival, and immune response were downregulated, while the upregulated cluster included largely uncharacterized processes. We propose that loss of *EGR3* regulation mediates synaptic deficits by targeting the synaptic vesicle cycle. Our results highlight the utility of integrating protein interactions with gene perturbations to generate a comprehensive framework for characterizing alterations in the molecular network as applied to AD.

In Brief

*Correspondence: rrissman@ucsd.edu.

AUTHOR CONTRIBUTIONS

Conceptualization, S.C. and R.A.R.; Methodology, S.C. and B.R.; Formal Analysis, S.C., S.B.R., R.S., and K.M.F.; Validation, S.C.; Writing - Original Draft, S.C.; Writing - Review & Editing, S.C., S.B.R., R.S., K.M.F., P.L.D.J., D.A.B., and R.A.R.; Visualization, S.C., D.M., and S.B.R.; Funding Acquisition, R.A.R.

DECLARATION OF INTERESTS

The authors declare no competing interests.

SUPPLEMENTAL INFORMATION

Supplemental Information can be found online at https://doi.org/10.1016/j.celrep.2019.06.073.

Canchi et al. reveal the transcriptomic dynamics of clinically and neuropathologically confirmed Alzheimer's disease subjects by integrating brain tissue-specific proteome data with gene network analysis. They identify perturbed biological processes and provide insights into the interactions between molecular mechanisms in symptomatic Alzheimer's disease.

Graphical Abstract

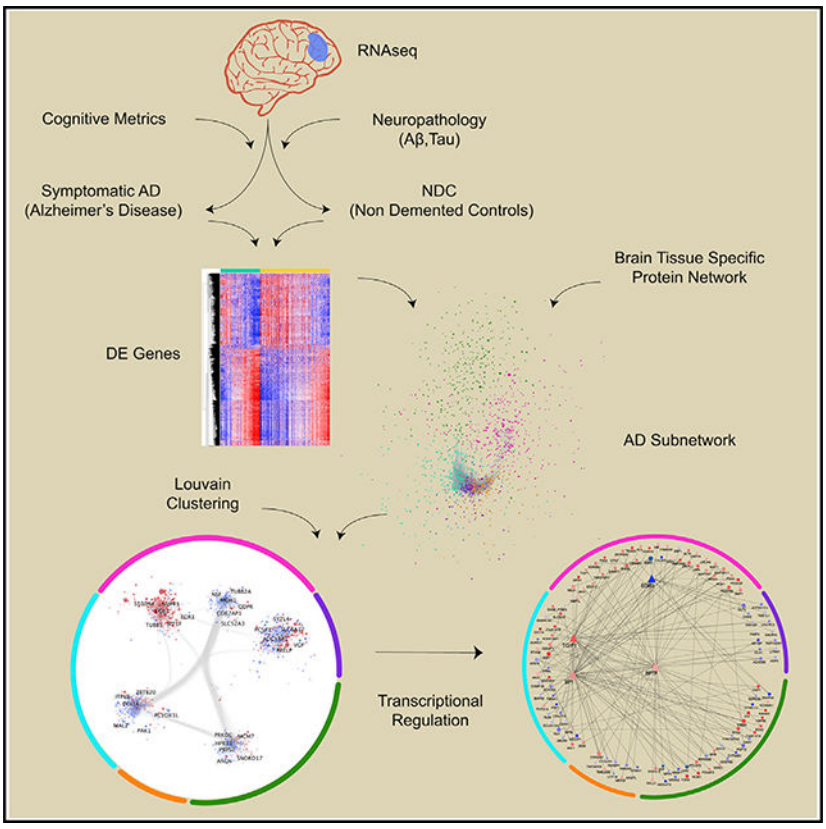

INTRODUCTION

An increase in the aging population with improved longevity reinforces the urgency for prevention and treatment of progressive neurodegenerative diseases including Alzheimer's disease (AD), the most common cause of dementia (Bloudek et al., 2011; Hyman et al., 2012). Although the predominant pathology of AD is accumulation of neuritic β-amyloid (Aβ) plaques and neurofibrillary tangles containing phosphorylated tau protein, cooccurrence of other neuropathological features is increasingly recognized to be a frequent event in brains of demented patients (Adlard et al., 2014; Bloudek et al., 2011). These changes, including inflammation, neuronal and synaptic loss, problems with blood circulation, and atrophy, correlate with clinical symptoms of cognitive decline and have led to changes in diagnostic criteria during the last decade (Bennett et al., 2012; Hyman et al., 2012; Sheng et al., 2012).

Multiple causal factors underlie the complexity of sporadic AD. Primary risk factors include age, gender, and family history (Hyman et al., 2012). The presence of elevated blood cholesterol, diabetes, depression, and multiple lifestyle and dietary factors is also associated with increased risk of AD dementia, although not necessarily with AD pathology (Bennett et al., 2012). Genetic mutations in amyloid precursor protein (*APP*), presenilin 1 (*PSEN1*), and presenilin 2 (*PSEN2*) associated with autosomal dominant AD were critical in identifying pathogenic mechanisms associated with Aβ accumulation (Bennet et al., 2011; Tan et al., 2014). Although many genome-wide association study (GWAS)-identified genes, including the ε4 allele of apolipoprotein E (*APOE*), have implications for Aβ and tau processing, most risk loci associate strongly with pathways involved in inflammation, lipid metabolism, and endocytosis, which may partially explain the association of non-genetic risk factors (Jones et al., 2015; Zhang et al., 2013). Translation of molecular insights into predictive screening and diagnosis is important, because clinical diagnosis of AD is difficult and often imprecise (Hyman et al., 2012). This is complicated by genetic mutations explaining only a small proportion of autosomal dominant AD and the presence of *APOE ε4* being insufficient to cause AD (Bennett et al., 2012; Bloudek et al., 2011; Hyman et al., 2012). In addition, considering the variability in the rate of cognitive decline among individuals, transcriptomic changes between symptomatic and asymptomatic AD subtypes may be distinct and warrant subject selection refinement (Bloudek et al., 2011; White et al., 2017).

In this study, we selected 414 clinically and neuropathologically confirmed AD subjects and cognitively normal age-matched controls, all sampled from a large, well-characterized community-based neuropathological study (Bennett et al., 2012; Mostafavi et al., 2018; Table 1). Integration of gene perturbations with protein interactions is a powerful method to identify the genes causing a phenotype that are functionally cohesive, interact physically, and share coherent biological pathways (Mitra et al., 2013). We characterize the molecular network dysregulation in AD relative to controls by integrating global gene expression profiles with a precalculated brain tissue-specific protein-protein interactome (Greene et al., 2015). Human brain transcriptome has revealed intrinsic topological organization of clusters of densely interconnected functional coexpressed modules (Jones et al., 2015; Mitra et al., 2013; Zhang et al., 2013). Detection of the intrinsic structure of a complex network such as the human brain transcriptome is typically addressed using community detection approaches, in which “community” refers to a collection of nodes that are more densely connected compared with nodes outside the community. These previous studies considered single-interaction data as a basis for identifying the hierarchical organization. In this study, we integrate the transcriptomic changes underlying AD with brain tissue-specific protein interaction networks to identify functional composite clusters by implementing the Louvain algorithm. We characterized the distinct gene clusters that revealed extensive expression changes across multiple biological and cellular pathways implicated in AD. By applying the strategy of gene set enrichment, we identify four transcriptional regulators across all clusters. These include transforming growth factor β (TGF-β)-induced factor homeobox 1 (*TGIF1*) and early growth response 3 (*EGR3*), which were previously not associated with AD and were validated by protein analysis of brain tissue samples from an independent AD cohort. We propose that loss of regulation of *EGR3,* which is crucial for short-term memory, mediates synaptic deficits by targeting the synaptic vesicle cycle (Poirier et al., 2008; Sheng

et al., 2012). These results highlight the utility of the integrated network approach to provide insights into global changes in gene interactions in complex heterogenous diseases such as AD.

RESULTS

Refined AD Phenotype Reveals Perturbation in the Transcriptomic Landscape

After adjusting for covariates and multiple testing, 1,722 genes were significantly differentially expressed in AD compared with age-matched non-demented controls (NDCs), and 57% of those genes were downregulated (Figure 1A; Table S1). Gene set enrichment analysis (GSEA) (Subramanian et al., 2005) revealed functional enrichment of specific biological processes (Gene Ontology [GO]) and molecular pathways (Kyoto Encyclopedia of Gene and Genomes [KEGG]) underlying these genes. A total of 453 upregulated and 113 downregulated MSigDB gene sets (Subramanian et al., 2005) were identified at a 5% false discovery rate (FDR). Among the GO terms that were enriched, those related to neural development, gliogenesis, metabolism and localization of proteins, and extracellular structure organization were upregulated, while those related to synaptic transmission, mitochondrial and metabolic processes, and extracellular transport were downregulated (Tables S2 and S3). These results are consistent with previous findings of multiple studies associating AD pathophysiology with genetic perturbation, and they demonstrate the complexity of the disease (Bloudek et al., 2011; Jones et al., 2015; Mostafavi et al., 2018; White et al., 2017; Zhang et al., 2013).

A total of 133 differentially expressed genes were also mitochondrial genes, defined as mitochondrial encoded genes from MitoCarta 2.0 (Calvo et al., 2016) (Figure 1B; Table S4). Among these are nuclear-encoded genes for oxidative phosphorylation (OXPHOS) (Figure 1C). These include NADH ubiquinone oxidoreductase core subunits S1 (*NDUFS1,* posterior error probability [PEP] = 2.4e–2), A5 (*NDUFA5,* PEP = 8.0e–5), A10 (*NDUFA10,* PEP = 1.3e–2), and B5 (*NDUFB5,* PEP = 2.4e–2), all part of complex I involved in transfer of electrons to the respiratory chain. Reduced expression of complex V genes, including ATPase inhibitory factor I (*ATPIF1,* PEP = 2.4e–3), subunit B (*ATP5F1,* PEP = 1.8e–3), and subunit F1 alpha (*ATP5A1*, PEP = 3.7e–2) have implications for production of ATP from ADP (Chaban et al., 2014). In addition, expression of 8 mitochondrial ribosomal protein (*MRP*) subunits involved in translation of the mitochondrial-encoded OXPHOS genes is downregulated. Downregulated nuclear and mitochondrial genes encoding subunits involved in OXPHOS have been shown in the brain and blood of subjects with AD and mild cognitive impairment (MCI) compared with NDCs (Devi et al., 2006; Lunnon et al., 2017). Although most mitochondrial genes were downregulated, 27 genes showed upregulation (Figure 1B). Of these, increased expression of diazepam-binding inhibitor (*DBI,* PEP = 8.9e–4), known for its role as a mediator in corticotropin-dependent adrenal steroidogenesis and in modulation of the action of the γ-aminobutyric acid (GABA) receptor, has been shown to be dose dependent on Aβ aggregates (Luchetti et al., 2011).

Aggregate Network of Protein and Genetic Interactions Reveals Gene Candidates in Biologically Distinct Clusters Associated with AD Pathogenesis

The AD subnetwork was first generated by integrating the differentially expressed genes into the Genome-Scale Integrated Analysis of Networks in Tissues (GIANT) brain-specific interactome (Greene et al., 2015). The inherent clustering structure of the AD subnetwork was identified computationally using the Louvain modularity maximization algorithm (Blondel et al., 2008) (Figure 2A). This graph-based, unsupervised clustering analysis does not require explicit assumptions and instead uses an iterative process to optimally partition nodes in a graph by maximizing the number of edges within clusters and minimizing the number of edges between clusters.

The largest connected AD subnetwork of 1,383 differentially expressed genes partitions into 8 distinct clusters ranging from 2 to 373 genes. We restricted our analysis to clusters containing at least 5 genes. There are fewer genes in the AD subnetwork than in the differentially expressed genes list, because the interactome is not complete. That is, not all differentially expressed genes were contained in the interactome. Many of these clusters are significantly upregulated or downregulated in AD with respect to NDCs (Figure 2B; Table S5). The AD subnetwork is uploaded to the Network Data Exchange (NDEx) platform for further visual and interactive exploration (see Supplemental Information for details). Three metrics were used to assess significance of up- and downregulation. The first metric was a simple binomial test, comparing the number of observed positive nodes within each cluster to the number expected given the rate of positive nodes within the full AD subnetwork. The second metric was the Kolmogorov-Smirnov test to check whether the distribution of log fold change expression values in each cluster is significantly different from the distribution in the full AD subnetwork (Figure 2B). The third metric was the Wilcoxon rank-sum test to check the relative shift in the distribution of the log fold change of expression values in each cluster when compared with the full distribution in the AD subnetwork. Of the 8 detected clusters, 5 that contained at least 5 genes were significantly enriched for up- or downregulated genes (Figure 2C; Tables S5 and S6). In addition to the gene-level tests at the network level, we assessed the patient-level distribution of expression in each cluster for both AD and NDC groups (Figure S2). The expression across all genes in a given cluster for each patient was averaged, and the distributions between AD and NDC groups were compared using a Wilcoxon rank-sum test. The patient-level results are consistent with the gene-level results.

Overrepresentation analysis of the genes in the clusters characterized significantly enriched biological processes and molecular pathways. This revealed functionally distinct units related to broad categories of synaptic transmission, signal transduction, cell survival and viability, immune response, and metabolism (Figure 3; Figures S1–S5; Table S7). The expression for clusters corresponding to synaptic transmission, DNA repair, immune response, and metabolism were downregulated, while the cluster with overall upregulation had many uncharacterized genes (Figure 2C). Although the cluster with immune response functional enrichment has a large set of downregulated genes, the set of upregulated genes in the cluster correspond to increased proinflammatory response. The downregulated genes within these pathways correspond to signaling components that promote cell survival,

immune homeostasis, phagocytosis, and metabolism. Although evidence points toward the role of innate immunity in driving the neuroinflammation in AD, the consequences of engaging adaptive immunity in AD pathogenesis are not completely understood. Ligation of CD28 is critical for effective functioning of conventional T cells and is crucial to mediating immunity checkpoints through competing pro- and anti-inflammatory effects. Decreased CD28 costimulation pathways as observed here, in concert with changes in signaling characteristics of the innate immune cells, support discovery of a disease-associated molecular signature of immune cells in the brain (Deczkowska et al., 2018; Marsh et al., 2016).

Cluster 0: Synaptic Transmission—Loss of neurons and synapses in the hippocampus and cerebral cortex, a characteristic of AD, is shown to strongly correlate with cognitive impairment, high levels of Aβ production, and tau oligomers (Sheng et al., 2012). Pathways in cluster 0 were enriched for neurotransmitter-related signaling (Figure 3; Figure S3; Table S7). Expression of neuregulin-1 (*NRG1,* PEP = 6.7e–4) and neurexin 3 (*NRXN3*, PEP = 4.6e–3), which promote the formation of functional synaptic structures, was downregulated (Martinez- Mir et al., 2013). Expression for $GABA_A$ receptors was downregulated and is comparable to evidence of decreased amplitude of GABA currents on examination of the electrophysiological activity of AD brains, which correlated with reduced mRNA and protein expression of α1 and γ2 GABA receptor subunits in the temporal cortex (Limon et al., 2012; Luchetti et al., 2011). Downregulation in glutamate ionotropic receptor α-amino-3-hydroxy-5-methyl-4-isoxazolepropionic acid (AMPA) subunits (*GRIA2, GRIA3,* and *GRIA4*) and kainate-type subunits (*GRIK1* and *GRIK2*), along with *SHANK2,* which forms a postsynaptic scaffold for receptor complexes, is consistent with the idea that excess Aβ can enhance endocytic internalization of AMPA and NMDA receptors and suppress long-term potentiation (LTP) in AD (Sheng et al., 2012). Increased expression of lysophosphatidic acid receptor 1 (*LPAR1,* PEP = 4.4e–3) a G protein-coupled receptor has been shown to regulate glutamatergic and GABAergic signaling, although the details are unclear (Yung et al., 2015).

In addition to neurotransmitters, neurosecretory proteins and neuropeptides are known for their role in neuronal cell communication. Reduced expression of neurosecretory protein VGF nerve growth factor inducible (*VGF,* PEP = 2.9e–5), associated with synaptic plasticity and function, has been identified in cerebrospinal fluid (CSF) and parietal cortex of AD patients (Cocco et al., 2010; Hendrickson et al., 2015). These results confirm and extend the trend to prefrontal cortex in AD. Based on the specificity of VGF to the CNS, it is an ideal candidate, with potential as a blood-based biomarker for AD. Reduced cortical corticotropin-releasing factor immunoreactivity (*CRF*, PEP = 2.1e–4) in the face of increased hypothalamic expression is a prominent neurochemical change in AD and is shown to mediate stress-induced hyperphosphorylated tau through its receptor 1 (*CRFR1*), with antagonist reduction of Aβ levels in animal AD models (Rissman et al., 2007; Zhang et al., 2016). Decreased expression of doublecortin-like kinase 1 (*DCLK1,* PEP = 7.7e–3), which has both microtubule-polymerizing activity and protein kinase activity, likely has implications for axon trafficking deficits (Koizumi et al., 2017). Downregulation of

dipeptidyl-peptidase 6 (*DPP6,* PEP = 1.5e–2) is associated with reduced dendritic spine density, a phenotype observed in AD brains (Lin et al., 2013).

Cluster 1: DNA Repair and Transcription—Abnormal cell-cycle reentry in response to accumulation of damaged DNA is hypothesized to precede AD pathogenesis (Davydov et al., 2003; Weissman et al., 2007). Pathways in cluster 1 were enriched for DNA replication and transcription (Figure 3; Figure S4; Table S7), with approximately 15% of genes associated with cell-regulated DNA repair and chromatin remodeling (Mjelle et al., 2015). One of the highly connected genes in this cluster, minichromosome maintenance complex component 7 (*MCM7,* PEP = 9.3e–5), was identified as an additional AD-susceptible locus in a large-scale GWAS study (Escott-Price et al., 2014). Expression of DNA-dependent protein kinase (*PRKDC,* PEP = 9.5e–3), which is essential for the repair of double-strand breaks, a lethal form of DNA damage, was downregulated and is comparable to protein expression observed in AD brains (Cardinale et al., 2012; Davydov et al., 2003). Reduction in the base excision repair, a multistep DNA repair pathway, has been detected in early stages of the disease (amnestic MCI), with a continued trend with progression to AD (Weissman et al., 2007). Reduced expression of tyrosyl-DNA phosphodiesterase 1 (*TDP1,* PEP = 4.0e–2), a DNA repair protein involved in base excision repair, is a rational result (El-Khamisy et al., 2005). Overexpression of the DEK proto-oncogene (*DEK,* PEP = 4.1e–2), known for its role in p53 destabilization, is associated with multiple cancer phenotypes and has not been characterized in AD with potential as an early target for neuronal homeostasis (Feng et al., 2017). PHD finger protein 19(*PHF19*, PEP = 3.1e–5), a Polycomb-like protein, is known to specifically bind to histone H3 lysine 36 trimethylation (H3K36me3) and is crucial for *PRC2* recruitment to CpG islands, which mainly mediate transcriptional repression (Brien et al., 2012). Although its role in AD remain unclear, overexpression of *PHF19* as observed here has been shown to correlate positively with astrocytoma grades (Li et al., 2013). Whether this was a consequence of cell-state activity or an essential event is to be determined. Although not directly linked to AD, suppression of chromatin assembly factor I (*CHAF1B*, PEP = 2.0e–3) has been shown regulate somatic cell identity in a transcription factor-induced cell-fate transition correlated to protein levels in Down syndrome brains and identified via whole exome sequencing to be associated with neurogenetic disorders with intellectual disability (Alazami et al., 2015; Cheloufi et al., 2015). Stathmin (*STMN1,* PEP = 3.3e–2) known to negatively correlate with neurofibrillary tangles and highly connected to genes in this cluster, is shown to mediate cell-cycle regulation via *MELK* kinase and has been investigated as a biomarker of DNA damage in AD (Marie et al., 2016; Watabe-Rudolph et al., 2012). This could provide an important link between dysregulation of microtubule polymerization and cell-cycle dynamics as seen in AD and merits further investigation.

Cluster 2: Immune Response—Immune system pathways were enriched in cluster 2 (Figure 3; Figure S5; Table S7). Several lines of evidence suggest that chronic neuroinflammation, shown to correlate with disease progression, could contribute to the pathogenesis of AD (Jones et al., 2015; Marsh et al., 2016; Zhang et al., 2013). The associated causal regulators, including *TYROBP* as described in Zhang et al. (2013), were not significant, although pathways under the Fc and Complement immune and microglia

modules are enriched. While the role of C-type lectin receptors (CLRs), members of the pattern recognition receptor family in AD, are unclear, two functional variants of mannose-binding lectin (*MBL2*), a soluble CLR, are associated with AD risk (Sjölander et al., 2013). Antagonists to *MBL2* have been shown to facilitate a favorable outcome in experimental models of traumatic brain and spinal injury, suggesting a potential target for modulation of immune response (De Blasio et al., 2017; Gensel et al., 2015). Increased expression of chemokine receptor 4 (*CXCR4,* PEP = 3e–0.2) is shown to be associated with higher levels of activated phosphorylated protein kinase C and with synaptic pruning in early development (Matcovitch-Natan et al., 2016; Weeraratna et al., 2007). This was concomitant with decreased expression of C2H2 zinc-finger protein (*PLAGL1,* PEP = 4.2e–7) known to activate SOCS3, a suppressor of cytokine signaling (Schmidt-Edelkraut et al., 2013). Fc receptor-mediated glial cell activation, identified as one of the immune pathways in AD GWAS study, has been attributed to adverse side effects associated with failed AD immunotherapy trials, reiterating the need to understand the functional roles of these receptors (Fuller et al., 2014; Jones et al., 2015). Decreased expression of a bromodomain family member (*BRWD1,* PEP = 1.7e–6), a histone reader essential for B lymphopoiesis, is in lieu of the observed loss of the cross talk between the innate immune system of the brain and the adaptive immune system facilitated by circulating B and T cells (Mandal et al., 2015; Marsh et al., 2016).

Cluster 3: Uncharacterized Gene Candidates—Genes from cluster 3, the only cluster with an overall upregulation in differential expression, were not readily characterized. No enriched pathways were detected, and only a few marginally significant GO terms were found. Examination of this cluster revealed more uncharacterized genes than expected by chance ($p < 0.05$), suggesting genes within this cluster would be attractive candidates for follow-up studies, because many encode for proteins not previously characterized or associated with AD. Enriched biological processes included small guanosine triphosphatase (GTPase)-mediated signal transduction (FDR = 6.21e–5), which is known to control diverse cellular activities (Figure S1). Evidence suggests that dysregulation of Rho- GTPase, specifically *RHOA-, RAC1* -, and CDC42-mediated actin dynamics, could be a key contributor to synaptic deficits observed in AD, yet interactions among the different signaling pathways remain unclear (Hooff et al., 2010). Ras homolog family members C (*RHOC,* PEP = 4.5e–2), D (*RHOD,* PEP = 9.5e–3), and G (*RHOG,* PEP = 1.2e–3) were upregulated, and increased expression of ras-associated protein rab13 (*RAB13,* PEP = 4.9e–3), a paralog for RAB8B, is consistent with the protein levels measured in AD brains (Hooff et al., 2010). ADP ribosylation factor subfamilies (*ARF3* and *ARF5*) of GTPase have critical roles in the secretory pathway for intracellular endoplasmic reticulum (ER)-Golgi trafficking and in vesicle formation (Hooff et al., 2010). *ARF6,* a paralog of *ARF3,* was reported to be an important modulator of *BACE1* sorting in early endosomes in a clathrin-independent route; abrogating its function led to increased Aβ secretion, while functions of *ARF5* in AD are unknown (Sannerud et al., 2011). AD GWAS-identified gene families, including *INPP5D, NME4, ABCA2,* and *PLXNB1*, were upregulated (Zhang et al., 2013). Transcription factor EB (*TFEB*), a master regulator for lysosomal biogenesis, was over-expressed, which is associated with regulated autophagy (Settembre et al., 2011). Given that

the events in AD are non-linear, whether the observed changes are pathogenic or protective is to be determined.

Cluster 4: Metabolism and Bioenergetics—Metabolic dysfunction is a well-established characteristic of AD, and pathways in cluster 4 were enriched for energy metabolism and vesicle-mediated transport (Figure 3; Figure S6; Table S7). Clinical imaging modalities have consistently shown brain glucose hypometabolism to be an early irregularity in patients with cognitive impairment and in some cases prelude memory deficits (Adlard et al., 2014; Bloudek et al., 2011). An increase in free radical production, a decrease in the ATP/ADP ratio, and an increased rate of oxidant damage to lipids, proteins, and mitochondrial DNA characterize the mitochondrial dysfunction in AD (Atamna and Frey, 2007; Tramutola et al., 2017). Whether mitochondrial dysfunction is induced by Aβ or an independent upstream process is unresolved. Reduction in expression of dynamin 1-like protein (*DNM1L,* PEP = 1.4e–3) is consistent with the observation that mitochondrial dynamics shift in favor of fission and depend on Aβ overexpression as seen in AD (Atamna and Frey, 2007). Increased fission could also be explained by reduced expression of hypoxia-inducible domain family member 1A (*HIGD1A,* PEP = 1.4e–2), shown to regulate mitochondrial fusion by inhibiting cleavage of *OPA1* (An et al., 2013). It has also been attributed to regulation of the mitochondrial γ-secretase, a multi-subunit protease complex known to cleave numerous transmembrane proteins, including notch and *APP*, and whose activity is dysregulated in AD (Hayashi et al., 2012). The presence of *APP* in the mitochondria is associated with reduced cytochrome *c* oxidase (*COX10,* PEP = 3.8e–5), which is essential for COX assembly and function of complex IV of the electron transport chain (Devi et al., 2006). Although the direct inhibition of COX on Aβ deposition has shown conflicting results in animal and cell culture models (Fukui et al., 2007; Silva et al., 2013), reduced expression of COX may lead to reduced regulatory heme, a key metabolite shown to bind with Aβ (Atamna and Frey, 2007). *HIGD1A* also plays the role of positively regulating the COX complex, presenting with a therapeutic treatment strategy applicable across various disorders with dysfunctional OXPHOS activity, including AD (Hayashi et al., 2015; Lunnon et al., 2017). The expression of malate dehydrogenase 1 (*MDH1,* PEP = 7.0e–3), a key enzyme in the tricarboxylic acid (TCA) cycle that reversibly catalyzes the oxidation of malate to oxaloacetate, was reduced, contrary to previous reports of increased protein expression (Atamna and Frey, 2007; Tramutola et al., 2017). This could reflect variance in methodological approaches, patient demography, or preferential transcription for this gene. Decreased *MDH1* expression is proposed to enhance oxidative stress and mitochondrial damage because of its interaction with *AKT1,* activating a cascade of pathway alterations implicated in AD, Parkinson's disease (PD), and amyotrophic lateral sclerosis (ALS) (Recabarren and Alarcón, 2017).

Apart from bioenergetics, alterations in metabolic pathways are observed and associated with risk of developing AD. Increased expression of the solute carrier family of riboflavin transporters (*SLC52A3,* PEP = 3.6e–2) is intriguing, considering riboflavin is a precursor to the complex II substrate flavin adenine dinucleotide. Findings of mutations and deficiency of the brain-specific transporter SLC52A3 are linked to motor neuron diseases (Brown-Vialetto-Van Laere syndrome and Fazio-Londe disease) (Bosch et al., 2011; Manole et al.,

2017), while its overexpression was shown to enhance the proliferatory capability of human glioma, mediating its effect through suppression of proapoptotic proteins and upregulation of matrix metalloproteinases (MMPs), specifically MMP-2 and MMP-9, which have been shown to correlate with both CSF Aβ and tau levels from AD patients (Fu et al., 2016; Wang et al., 2014). Understanding the signaling pathways of *SLC52A3* warrants further research for validity as clinical diagnostic markers and for dietary considerations (Jones et al., 2017). Adiponectin receptor 1 (*ADIPOR1*, PEP = 8.4e–4), which transduce signals from adiponectin, an adipocyte-derived hormone involved in control of fat metabolism and insulin sensitivity, was upregulated. Because of its relatively recent discovery, data on *ADIPOR1* gene expression in AD are lacking, although increased plasma and CSF adiponectin has been detected in MCI and AD patients (Thundyil et al., 2012).

Regulatory Mechanisms of AD Pathogenesis Include TGIF1 and EGR3

We identified four transcriptional regulators whose targets were significantly enriched in the AD subnetwork and that were differentially expressed across all clusters (Table S8). Using the overrepresentation analysis feature of the pathway analysis tool WebGestalt, with a background set of all expressed genes in the data, we identified transcription factors that had more targets in the AD subnetwork than would be expected by chance. Of these significantly enriched transcriptional regulators, two were strongly significantly differentially expressed (*SP1* and *EGR3,* adjusted $p < 0.05$) and two were marginally significantly differentially expressed (*TGIF1* and *BPTF,* adjusted $p < 0.30$) (Figure 4; Figure S7). Specificity protein 1 (*SP1*) is dysregulated in AD and can regulate key genes associated with AD pathology, i.e., *APP,* tau, and *APOE* (Citron et al., 2008). Gene members of the early growth response family (*EGR3* and *EGR1*) are zinc-finger transcription factors essential for synaptic plasticity and memory and are downregulated. Dysregulation of *EGR1,* a critical microglial homeostatic gene required for maintenance of LTP, was associated with pathogenesis of APP-expressing mice, while *EGR3,* critical for short-term memory, has not been previously associated with AD (Koldamova et al., 2014; Matcovitch-Natan et al., 2016; Poirier et al., 2008). *BPTF/FAC1* is a chromatin remodeler first identified in AD brain whose overexpression is associated with apoptotic cell death (Strachan et al., 2005). *TGF-β* and bone morphogenic protein (*BMP*) bind via receptors (*TGFBR1, TGFBR2, TGFBR3,* and *BMPR2*) and activate Smad to regulate gene expression (Massague, 2012). Transcriptional corepressor *TGIF* recruits histone deacetylase (*HDAC*) to modulate Smad complexes to control the *TGF-β* signaling-based activation; these complexes have pleiotropic functions and are disrupted in AD (von Bernhardi et al., 2015).

TGF-β signaling across multiple cell types can activate several Smad-dependent and Smad-independent pathways, including mitogen-activated protein kinases (MAPKs), nuclear factor κB (NF-κB), and phosphatidylinositol 3-kinase (PI3K)/AKT, with contradictory results in a context-dependent manner. Consistent with observations in AD brains, overexpression of *TGF-β* and its receptors associated with increased Aβ accumulation, along with downregulation of *BMPR2,* point toward dysregulation in signaling mediated by *TGF-β* (von Bernhardi et al., 2015). Downregulation of *BMPR2* observed here could be primarily mediated by downregulation of *EGR1,* an essential microglial transcription factor (Matcovitch-Natan et al., 2016). Deficiency in *BMPR2* is linked to increased sensitivity to

DNA damage, along with alterations in DNA repair efficiency, and upregulated *SP1* could reflect DNA damage control (Li et al., 2014). This could provide an important link between neurodegenerative microglial phenotype and DNA damage observed in AD.

Downregulation of nemo-like kinase (*NLK*) and upregulation of *NOTCH4,* which is shown to strongly couple to AD risk genes and its downstream coactivator complex *RBPJ,* point toward ectopic cell-cycle reactivation (Bennet et al., 2011; Brai et al., 2016). Surprisingly, these observations coincide with dysregulation of genes involved in reprogramming of cell function, i.e., *KLF9* is downregulated, while *SOX2, SALL2,* and *JUND* are up- regulated, consistent with reduced efficacy of glucocorticoids (GCs) in the aging brain (Juszczak and Stankiewicz, 2017). Downregulated *KLF9* and upregulated *JUND* and *SALL2* promote cell proliferation and activate PI3K/AKT pathways involved in growth factors, while increased expression of *SOX2* and *SOX12* can act synergistically with octamer-binding proteins (*POU3F2* and *POU3F3*) to implement a feedforward circuit to increase expression of genes (*YES1* and *ID4*) associated with cell reprogramming. Increased expression of *SGK1,* regulated by *BPTF,* could stem from *TGF-β*-activated PI3K signaling, leading to enhanced activity of NF-κB and providing positive feedback through cross talk between the two pathways (Juszczak and Stankiewicz, 2017; Massagué, 2012).

Protein Expression of TGIF1 and EGR1 Is in Concordance with Transcript-Level Expression

To substantiate the differences in transcription between AD and non-demented aged brains, we assessed the protein expression of *TGIF1* and *EGR1*, the direct target for *EGR3,* in prefrontal cortex of AD and age-matched control brains from an independent cohort. *EGR1* shares structural and functional homology with *EGR3* and reportedly is dysregulated in AD brains, correlating with severity of cognitive decline (Zhu et al., 2016). In line with changes in the transcriptome data, we observed an overall 72% decrease in *EGR1* and a 51% increase in *TGIF1* levels in AD brains relative to NDCs, and these trends reached statistical significance (Figure 5). We found *EGR1* and *TGIF1* distribution across all cell types in the control brains and *EGR1* protein levels were particularly diminished in pyramidal neurons in AD brains. Overall, these results are consistent with the direction of change at mRNA levels, along with the strength of association in AD relative to NDCs.

DISCUSSION

We employed the Louvain modularity maximization algorithm, an unbiased and unsupervised community detection method, to identify coherent functional clusters in the molecular network associated with clinical and pathological AD when compared with age-matched NDCs. A key feature of this study is the integration of brain tissue-specific protein interactions with gene expression profiles derived from large sampling of postmortem transcriptome data, which help strengthen disease associations. This approach and our study allowed identification of distinct biological clusters that point toward associations critical for AD (Blalock et al., 2004; Davydov et al., 2003; Jones et al., 2015; Mostafavi et al., 2018; Tramutola et al., 2017; Zhang et al., 2013). We found the average global expression for clusters that broadly correspond to synaptic transmission, metabolism, cell cycle and

survival, and immune response was downregulated, while upregulated cluster 3 had a large set of uncharacterized pathways and processes. By refining the subject selection, we identified genes with target potential, confirmed some previous correlations, and found a lack of associations for other previously reported GWAS-computed AD-susceptible genes.

The fundamental finding of this study is the identification of sets of coexpressed genes, with inherent expression distribution corresponding to discrete biological processes to be associated with symptomatic AD. We identified transcriptional regulators across all clusters, including *EGR3* and *TGIF1,* along with their coexpressed targets. We found downregulation of *EGR3* was associated with a dysregulated synaptic vesicle cycle and postulated to mediate synaptic deficits as seen in AD. Consistent with the association of synaptic loss with AD, we observed a concerted downregulation of many genes that code for proteins involved in the synaptic vesicle cycle, of which key genes are regulated by *EGR3* (Figure 6). Vacuolar ATPase (V-ATPase) is an essential proton pump highly expressed on the membrane of the presynaptic vesicle, facilitates neurotransmitter concentration in synaptic vesicles, and is differentially expressed in brains of different *APOE* isoforms (Woody et al., 2016). The C1 subunit of V-ATPase (*ATP6V1C1*) is crucial to connect the ATP catalytic domain (V_1) to the proton-translocation domain (V_0) and its downregulation has implications for vesicle acidification, as well as membrane fusion. Reduction in expression of neuronal SNARE synaptosome-associated protein 25 (*SNAP25*), along with synaptotagmins (*SYT5* and *SYT13*) and syntaxin-binding proteins (*STXBP1* and *STXBP5L*), indicates reduced vesicle docking and SNARE-mediated fusion (Bereczki et al., 2016). Furthermore, decrease in vesicle-fusion ATPase (*NSF*), necessary for disassociating the SNARE complex from the plasma membrane, implicates decreased availability of uncomplexed SNARE (Jahn and Scheller, 2006). Reduced clathrin (CLTC), along with adaptor protein complex (AP2A), synaptophysin (SYP), and rab (*RAB3A*), implies reduced vesicle recycling (Bereczki et al., 2016). Targeting the regulation of the dysfunction of *CLTC*-mediated endocytosis for a synaptic receptor holds promise as an early intervention strategy (Sheng et al., 2012). Neurosecretory polypeptide precursor *VGF* is enhanced in neuronal activity associated with LTP and can be postulated to have a role in the sorting of other regulated secretory proteins, including glutamate, in immature vesicles (Hendrickson et al., 2015). Sortilin-related receptor (*SORCS3*), a neuronal receptor for proteolytic processing of *APP*, is implicated in AD and is shown to modulate long-term depression (LTD; Breiderhoff et al., 2013). EGR3-mediated reductions in *VGF* and *SORCS3* aid in the observed phenotype of Aβ-induced impairment in LTP and neuronal networks (Sheng et al., 2012).

Although little is known about the potential contributions of *TGIF1* in AD, there is evidence of involvement of impaired TGF-β signaling in pathogenesis of AD (von Bernhardi et al., 2015). Gene targets directly repressed by *TGIF1* or indirectly repressed in conjunction with corepressors point to regulation of gene expression aimed at arresting the cell cycle (*CDKN2C, MAX, MXI1, WWC1,* and *TNS2*), repairing a DNA strand (*DDIT4, EYA2,* and *ZYMND8*), and restoring homeostasis (*CEP57* and *GAB2*). Increased expression of *TGIF1*-regulated syntaxin 4 (*STX4*), critical for vesicle docking, and the Wnt frizzled receptor (*FZD9*) and coreceptor (*LRP5*), which regulate the synaptic vesicle cycle, may be compensatory mechanisms to restore effects mediated by *EGR3* (Inestrosa and Varela-Nallar, 2014). Although the findings of the study are robust at the network level, more

detailed experiments and model system studies will provide clarity on the specific regulatory mechanisms.

It is important to consider some potential limitations of the interpretations of this study. The effect of rate of decline between the pathological subtypes in AD was not incorporated into the analysis. This could bias the differential gene significance toward genes with similar expression change in both subgroups relative to the NDCs. The underlying gene-gene interaction network used is imperfect. GIANT uses an algorithm to predict some gene-gene interactions, and although the data were thoroughly benchmarked, the algorithm is not perfect and there are likely numerous false-positive interactions. The clustering algorithm used partitions to annotate genes to a given cluster such that each gene could belong to only one cluster. Biologically, some genes may be involved in multiple functions, and that is not captured by this clustering algorithm. Functional enrichment analysis with pathway databases only captures known and established biology. Clusters or genes that are not significantly enriched may represent undescribed pathways or functions, but existing databases do not help with the interpretation of these pathways. RNA sequencing (RNA-seq) data used in the study was obtained from bulk tissue, which represents a heterogenous cellular mixture with known variability and changes in cellular composition with age and with AD. Some observed changes in the gene signals may reflect relative changes in cellular abundance rather than a true biological mechanism.

Altogether, our study highlights the potential for integrating brain-specific protein networks with transcriptome changes to identify key biological changes associated with symptomatic AD. We have demonstrated the use of the network approach to prioritize transcriptional regulators; expression patterns of a small subset of these regulators matched protein levels in brain tissue. *EGR3* and *TGIF1* identified in this pilot study are potential targets for AD therapeutics and require further detailed evaluation. Understanding detailed molecular changes in complex diseases such as AD is of prime importance, and future studies incorporating transcriptomic changes at the single cell may be able to address the cell-specific transcriptional dysregulation. The transcriptomic alterations listed in this study may represent an important resource for investigations of molecular mechanisms involved in symptomatic AD.

STAR★METHODS

LEAD CONTACT AND MATERIALS AVAILABILITY

Further information and requests for reagents and resources should be directed to and will be fulfilled by the Lead Contact, Robert A. Rissman (rrissman@ucsd.edu).

EXPERIMENTAL MODEL AND SUBJECT DETAILS

The Religious Orders Study and Rush Memory and Aging Project (ROSMAP) are an ongoing longitudinal clinical-pathologic cohort studies of aging and dementia with enrollment of aged individuals without known dementia at baseline (Bennett et al., 2012). All participants are organ donors. Participants undergo detailed annual clinical evaluation. At death, a postmortem brain evaluation is performed, including silver stain to assay AD

pathology (neuritic and diffuse plaques, and neurofibrillary tangles), and Aβ load by image analysis and the density of PHF tau-positive neurofibrillary tangles (Bennett et al., 2012). The Institutional Review Board of the Rush University Medical Center approved the both studies. An informed consent and an anatomical gift act are obtained from each participant, as is a repository consent that allows for sharing of data and biospecimens.

Subjects were classified as either non demented controls (NDC) or AD based on a weighted combination of complementary information including cognitive score (MMSE) within two years of death along with three separate pathological scores i.e., total amyloid load, neurofibrillary tangles (Braak stage), and presence of neuritic plaques (CERAD score) (Hyman et al., 2012). Non-demented controls (NDC) included cognitively intact subjects (no diagnosis of mild cognitive impairment within two years of death) containing diffuse amyloid deposits in absence of neuritic plaques, and neurofibrillary tangles confined to the entorhinal region of the brain. For subjects with cognitive impairment, AD diagnosis was assigned based on the high or intermediate likelihood of AD neuropathology as presented in the revised NIA-AA guidelines for neuropathologic assessment of disorders of the brain common in the elderly (Hyman et al., 2012). A total of 414 subjects who passed these criteria were included in the current study (Table 1). Assessment of the pathological metrics as well as the characteristics of the cohort has been previously described in detail (Bennett et al., 2012; Mostafavi et al., 2018).

For the validation cohort, subjects were selected based on diagnostic criteria as described above and brain tissue samples were obtained from University of California San Diego Shiley-Marcos Alzheimer's Disease Research Center (ADRC) brain bank. BA9 tissue samples were obtained from five non-demented aged controls (77.25 ± 15.2 years, 10.8 ± 2.7 hours, 60% M) and five AD subjects (80.6 ± 7.8 years, 9.4 ± 5.4 hours, 80% M). The experiment was done with the approval of the Institutional Review Board at the University of California San Diego.

METHOD DETAILS

ROSMAP RNA-seq Data—RNA was extracted from the gray matter of the dorsolateral prefrontal cortex using QIAGEN's miRNeasy mini kit (cat. no. 217004) and the RNase free DNase Set (cat. no. 79254). These samples were quantified by Nanodrop and quality was evaluated by Agilent Bioanalyzer. RNA-Seq library preparation included the strand specific dUTP method with poly-A selection on samples that met quality (Bioanalyzer RNA integrity (RIN) score > 5) and quantity thresholds (5ug). Sequencing was performed on the Illumina HiSeq with 101bp paired-end reads and achieved coverage of 150M reads of the first 12 samples. These 12 samples will serve as a deep coverage reference and included 2 males and 2 females of non-impaired, mild cognitive impaired, and Alzheimer's cases. The remaining samples were sequenced with coverage of 50M reads. The libraries were constructed and pooled according to the RIN scores such that similar RIN scores would be pooled together. Varying RIN scores results in a larger spread of insert sizes during library construction and leads to uneven coverage distribution throughout the pool.

The raw RNA-seq files were processed to trim the adaptor sequences and to remove rRNA reads. Using the non-gapped aligner Bowtie (Langmead et al., 2009), the reads were aligned

to reference transcriptome and RSEM (Li and Dewey, 2011) was utilized to estimate the transcript levels in the form of fragments per kilobase of exon per million reads mapped (FPKM). Details of the RNA-seq data pipeline can be found in previous literature (Mostafavi et al., 2018; White et al., 2017).

Immunohistochemistry for TGIF1 and EGR3—We assessed the protein expression and distribution of *TGIF1* and *EGR3* target *EGR1* in prefrontal cortex brain tissue of clinically diagnosed pathologically confirmed AD and from age matched controls using standard immunohistochemistry techniques. Paraffin-embedded tissue blocks were serially sectioned and incubated with either TGIF antibody (H-1) (Santa Cruz Biotechnology) or EGR1 antibody (Cell Signaling Technology). Staining was performed with chromogen 3,3' -diaminobenzidine (DAB) to identify the immunoreactive structures and counterstained with hematoxylin. All images were acquired using an upright microscope (Leica DM5500B) at a resolution of 1392 × 1040 pixels and consistent aperture and gain settings.

AD Subnetwork—The full AD subnetwork shown in Figure 2 has been added to the Network Data Exchange (NDEx) platform.

http://www.ndexbio.org/#/network/0f329e3e-c347-11e8-aaa6-0ac135e8bacf?accesskey=21fb4630b60dd2458204226de0be272fe327456ec147721ad362c16d3871723d

Alternatively, the network can also be obtained by searching the NDEx website for the unique network identifier UUID: 0f329e3e-c347–11e8-aaa6–0ac135e8ba*cf*.

Note that because there are more than 10,000 edges only a (very small) subset of the edges are shown on the NDEx website interface. Users can however download the full network and view in Cytoscape.

QUANTIFICATION AND STATISTICAL ANALYSIS

Gene Expression Analysis—Expression data were downloaded from ROSMAP as FPKM values and normalized using a multi-loess method and batch effects removed using COMBAT algorithm (Johnson et al., 2007). For the log-transformed expression data, linear regression models were fit to account for effects of diagnostic conditions as well as confounding covariates of age at death, sex, postmortem interval (PMI) and APOE status for the risk allele. Test for statistical significance was achieved by implementation of a Bayesian strategy of Lönnstedt and Speed as implemented in *R* package *limma* (Ritchie et al., 2015). Genes are sorted by their posterior error probability (PEP) and considered significant at PEP < 0.05.

Background Interactome—The background interactome on which the network analysis was conducted was built from the brain-specific network in the GIANT database (Greene et al., 2015). This network is composed of edges which support a strong tissue-specific functional interaction between source and target genes. This network, thresholded at an edge confidence of 0.2, contains 14,545 genes, and 1,370,174 edges, and represents genes and interactions which are likely to be present in normal brain function. The identified

differentially expressed genes were mapped onto this network to create an AD subnetwork. Network visualization was accomplished using visJS2Jupyter (Rosenthal et al., 2018).

Clustering analysis—Clusters were identified in the AD subnetwork using a network-based modularity maximization algorithm (Blondel et al., 2008). This algorithm, commonly referred to as the Louvain clustering algorithm, identifies groups of nodes which have many connections within groups, and few connections between groups, and is efficient at extracting community structure from large networks. The algorithm iteratively maximizes the modularity, Q, defined as follows:

$$Q = \frac{1}{2m}\sum_{i,j}\left[A_{ij} - \frac{k_i k_j}{2m}\right]\delta(C_i, C_j)$$

Where A_{ij} is the binary adjacency matrix element representing the presence or absence of the connection between node i and node j, k_i represents the degree of node i, where degree is defined as the number of nodes directly connected to node i, c_i is the community to which node i belongs, and the function $\delta(x, y)$ is 1 if $x = y$, and otherwise it is 0. m is the total number of edges in the network, $m = (1/2)\sum_{ij} A_{ij}$ (divided by two to avoid double counting). See Blondel et al. (2008) for more details on the algorithm.

The Louvain algorithm does not require selection or fine-tuning of parameters, as do some other clustering algorithms such as, K-means clustering and hierarchical clustering (such as are used in the WGCNA R package). Rather, clusters are determined by finding groupings of genes which have many within group connections, and few between group connections. This algorithm has proven useful in detecting modules, or clusters, in protein-protein interaction networks, such as the one used here (Fortunato, 2010; van Laarhoven and Marchiori, 2012).

Functional Annotation and Pathway Analysis—To identify the underlying biological functions enriched in AD, Gene Set Enrichment Analysis (GSEA) was implemented which identifies the enrichment of functionally defined gene sets using a modified Kolmogorov-Smirnov statistic (Subramanian et al., 2005). The Molecular Signature Database (MSigDb v6.0) (Subramanian et al., 2005) consists of well over 4000 gene sets from functionally well-established or published pathways from databases including Gene Ontology (GO), the Kyoto Encyclopedia of Gene and Genomes (KEGG), BioCarta, and Reactome. Statistical significance after adjusting for multiple testing is defined at FDR < 0.05. Gene set-based permutation test of 1000 permutations was applied. Detailed description of the GSEA algorithm, testing metrics and the implementation have been described previously (Subramanian et al., 2005). Hypergeometric test was utilized to test of statistical significance of the enriched biological process and pathways identified for the differential expressed genes in the clusters (Wang et al., 2017; Yu et al., 2012). Overrepresentation enrichment analysis was conducted using the full set of genes from the AD subnetwork as the reference gene set, corrected for multiple testing using the Benjamini-Hochberg procedure and FDR < 0.05 was considered significant.

Transcriptional Regulation Analysis—To identify transcription factors (TF) likely related to AD, we analyzed for enrichment of transcription factor targets in the AD clustered subnetwork (Wang et al., 2017). This resulted in 16 significantly enriched transcription factors (Table S8). We further filtered this list by differential expression in AD versus NDC, resulting in 4 candidate TFs. These four TFs are all significantly differentially expressed in AD as compared to NDC and have more targets than would be expected by chance in the AD subnetwork (Figure S7). The TF subnetwork is visualized to highlight the connections between TF and targets along with connections between targets using visJS2Jupyter (Rosenthal et al., 2018).

Quantification of Image Data: Images were analyzed in ImageJ software (Schneider et al., 2012). Custom designed macro was used to convert the optical images to grayscale, threshold and measure the TGIF or EGR1 positive area fraction relative to the optical field. Area fraction were averaged across image fields to generate within sample mean values for each sample in a given diagnostic group for each protein of interest. Due to the non-normal distribution of the data, test of significance was evaluated using Wilcoxon rank sum test and differences were considered significant when $p < 0.05$. GraphPad Prism 7 software was used for statistical analysis.

DATA AND CODE AVAILABILITY

RNaseq data reported in this paper are hosted on NIA supported AMP-AD knowledge portal on Synapse platform, and the accession number is Synapse: syn3388564 [https://doi.org/10.7303/syn3388564]. Additional data can be accessed from the Rush Alzheimer's Disease Center Resource Sharing hub (https://www.radc.rush.edu/).

Supplementary Material

Refer to Web version on PubMed Central for supplementary material.

ACKNOWLEDGMENTS

We gratefully acknowledge the study participants, tissue donations from UCSD and Rush Alzheimer's Disease Centers and their related funding sources (UCSD ADRC - AG062429/AG005131 and Rush ADC - AG10161). This study was funded by VA merit grant BX003040 and NIH grants AG18840, AG051839, and AG10483 (to R.A.R.) and partially supported by NIH grants UL1TR001442 of CTSA and P30AG10161, RF1AG15819, R01AG17917, and U01AG4652. The contents do not represent the views of UCSD, the U.S. Department of Veterans Affairs, NIH, or the U.S. government.

REFERENCES

Adlard PA, Tran BA, Finkelstein DI, Desmond PM, Johnston LA, Bush AI, and Egan GF (2014). A review of β-amyloid neuroimaging in Alzheimer's disease. Front. Neurosci 8, 327. [PubMed: 25400539]

Alazami AM, Patel N, Shamseldin HE, Anazi S, Al-Dosari MS, Alzahrani F, Hijazi H, Alshammari M, Aldahmesh MA, Salih MA, et al. (2015). Accelerating novel candidate gene discovery in neurogenetic disorders via whole-exome sequencing of prescreened multiplex consanguineous families. Cell Rep. 10, 148–161. [PubMed: 25558065]

An H-J, Cho G, Lee J-O, Paik S-G, Kim YS, and Lee H (2013). Higd1a interacts with Opa1 and is required for the morphological and functional integrity of mitochondria. Proc. Natl. Acad. Sci. USA 110, 13014–13019. [PubMed: 23878241]

Atamna H, and Frey WH 2nd. (2007). Mechanisms of mitochondrial dysfunction and energy deficiency in Alzheimer's disease. Mitochondrion 7, 297–310. [PubMed: 17625988]

Bennet AM, Reynolds CA, Eriksson UK, Hong MG, Blennow K, Gatz M, Alexeyenko A, Pedersen NL, and Prince JA (2011). Genetic association of sequence variants near AGER/NOTCH4 and dementia. J. Alzheimers Dis 24, 475–84. [PubMed: 21297263]

Bennett DA, Schneider JA, Arvanitakis Z, and Wilson RS (2012). Overview and findings from the religious orders study. Curr. Alzheimer Res 9, 628–645. [PubMed: 22471860]

Bereczki E, Francis PT, Howlett D, Pereira JB, Höglund K, Bogstedt A, Cedazo-Minguez A, Baek J-H, Hortobágyi T, Attems J, et al. (2016). Synaptic proteins predict cognitive decline in Alzheimer's disease and Lewy body dementia. Alzheimers Dement. 12, 1149–1158. [PubMed: 27224930]

Blalock EM, Geddes JW, Chen KC, Porter NM, Markesbery WR, and Landfield PW (2004). Incipient Alzheimer's disease: microarray correlation analyses reveal major transcriptional and tumor suppressor responses. Proc. Natl. Acad. Sci. USA 101, 2173–2178. [PubMed: 14769913]

Blondel VD, Guillaume J-L, Lambiotte R, and Lefebvre E (2008). Fast unfolding of communities in large networks. J. Stat. Mech 2008, P10008.

Bloudek LM, Spackman DE, Blankenburg M, and Sullivan SD (2011). Review and meta-analysis of biomarkers and diagnostic imaging in Alzheimer's disease. J. Alzheimers Dis 26, 627–645. [PubMed: 21694448]

Bosch AM, Abeling NGGM, Ijlst L, Knoester H, van der Pol WL, Stroomer AEM, Wanders RJ, Visser G, Wijburg FA, Duran M, and Waterham HR (2011). Brown-Vialetto-Van Laere and Fazio Londe syndrome is associated with a riboflavin transporter defect mimicking mild MADD: a new inborn error of metabolism with potential treatment. J. Inherit. Metab. Dis 34, 159–164. [PubMed: 21110228]

Brai E, Alina Raio N, and Alberi L (2016). Notch1 hallmarks fibrillary depositions in sporadic Alzheimer's disease. Acta Neuropathol. Commun 4, 64. [PubMed: 27364742]

Breiderhoff T, Christiansen GB, Pallesen LT, Vaegter C, Nykjaer A, Holm MM, Glerup S, and Willnow TE (2013). Sortilin-related receptor SORCS3 is a postsynaptic modulator of synaptic depression and fear extinction. PLoS ONE 8, e75006. [PubMed: 24069373]

Brien GL, Gambero G, O'Connell DJ, Jerman E, Turner SA, Egan CM, Dunne EJ, Jurgens MC, Wynne K, Piao L, et al. (2012). Polycomb PHF19 binds H3K36me3 and recruits PRC2 and demethylase NO66 to embryonic stem cell genes during differentiation. Nat. Struct. Mol. Biol 19, 1273–1281. [PubMed: 23160351]

Calvo SE, Clauser KR, and Mootha VK (2016). MitoCarta2.0: an updated inventory of mammalian mitochondrial proteins. Nucleic Acids Res. 44 (D1), D1251–D1257. [PubMed: 26450961]

Cardinale A, Racaniello M, Saladini S, De Chiara G, Mollinari C, de Stefano MC, Pocchiari M, Garaci E, and Merlo D (2012). Sublethal doses of β-amyloid peptide abrogate DNA-dependent protein kinase activity. J. Biol. Chem 287, 2618–2631. [PubMed: 22139836]

Chaban Y, Boekema EJ, and Dudkina NV (2014). Structures of mitochondrial oxidative phosphorylation supercomplexes and mechanisms for their stabilisation. Biochim. Biophys. Acta 1837, 418–426. [PubMed: 24183696]

Cheloufi S, Elling U, Hopfgartner B, Jung YL, Murn J, Ninova M, Hubmann M, Badeaux AI, Euong Ang C, Tenen D, et al. (2015). The histone chaperone CAF-1 safeguards somatic cell identity. Nature 528, 218–224. [PubMed: 26659182]

Citron BA, Dennis JS, Zeitlin RS, and Echeverria V (2008). Transcription factor Sp1 dysregulation in Alzheimer's disease. J. Neurosci. Res 86, 2499–2504. [PubMed: 18449948]

Cocco C, D'Amato F, Noli B, Ledda A, Brancia C, Bongioanni P, and Ferri G-L (2010). Distribution of VGF peptides in the human cortex and their selective changes in Parkinson's and Alzheimer's diseases. J. Anat 217, 683–693. [PubMed: 21039478]

Davydov V, Hansen LA, and Shackelford DA (2003). Is DNA repair compromised in Alzheimer's disease? Neurobiol. Aging 24, 953–968. [PubMed: 12928056]

De Blasio D, Fumagalli S, Longhi L, Orsini F, Palmioli A, Stravalaci M, Vegliante G, Zanier ER, Bernardi A, Gobbi M, and De Simoni M-G (2017). Pharmacological inhibition of mannose-binding lectin ameliorates neurobehavioral dysfunction following experimental traumatic brain injury. J. Cereb. Blood Flow Metab 37, 938–950. [PubMed: 27165013]

Deczkowska A, Keren-Shaul H, Weiner A, Colonna M, Schwartz M, and Amit I (2018). Disease-Associated Microglia: A Universal Immune Sensor of Neurodegeneration. Cell 173, 1073–1081. [PubMed: 29775591]

Devi L, Prabhu BM, Galati DF, Avadhani NG, and Anandatheerthavarada HK (2006). Accumulation of amyloid precursor protein in the mitochondrial import channels of human Alzheimer's disease brain is associated with mitochondrial dysfunction. J. Neurosci 26, 9057–9068. [PubMed: 16943564]

El-Khamisy SF, Saifi GM, Weinfeld M, Johansson F, Helleday T, Lupski JR, and Caldecott KW (2005). Defective DNA single-strand break repair in spinocerebellar ataxia with axonal neuropathy-1. Nature 434, 108–113. [PubMed: 15744309]

Escott-Price V, Bellenguez C, Wang L-S, Choi S-H, Harold D, Jones L, Holmans P, Gerrish A, Vedernikov A, Richards A, et al.; United Kingdom Brain Expression Consortium; Cardiovascular Health Study (CHS) (2014). Gene-wide analysis detects two new susceptibility genes for Alzheimer's disease. PLoS ONE 9, e94661. [PubMed: 24922517]

Feng T, Liu Y, Li C, Li Z, and Cai H (2017). DEK proto-oncogene is highly expressed in astrocytic tumors and regulates glioblastoma cell proliferation and apoptosis. Tumour Biol. 39, 1010428317716248. [PubMed: 28670979]

Fortunato S (2010). Community detection in graphs. Phys. Rep 486, 75–174.

Fu T, Liu Y, Wang Q, Sun Z, Di H, Fan W, Liu M, and Wang J (2016). Overexpression of riboflavin transporter 2 contributes toward progression and invasion of glioma. Neuroreport 27, 1167–1173. [PubMed: 27584688]

Fukui H, Diaz F, Garcia S, and Moraes CT (2007). Cytochrome c oxidase deficiency in neurons decreases both oxidative stress and amyloid formation in a mouse model of Alzheimer's disease. Proc. Natl. Acad. Sci. USA 104, 14163–14168. [PubMed: 17715058]

Fuller JP, Stavenhagen JB, and Teeling JL (2014). New roles for Fc receptors in neurodegeneration-the impact on Immunotherapy for Alzheimer's Disease. Front. Neurosci 8, 235. [PubMed: 25191216]

Gensel JC, Wang Y, Guan Z, Beckwith KA, Braun KJ, Wei P, McTigue DM, and Popovich PG (2015). Toll-Like Receptors and Dectin-1, a C-Type Lectin Receptor, Trigger Divergent Functions in CNS Macrophages. J. Neurosci 35, 9966–9976. [PubMed: 26156997]

Greene CS, Krishnan A, Wong AK, Ricciotti E, Zelaya RA, Himmelstein DS, Zhang R, Hartmann BM, Zaslavsky E, Sealfon SC, et al. (2015). Understanding multicellular function and disease with human tissue-specific networks. Nat. Genet 47, 569–576. [PubMed: 25915600]

Hagberg A, Swart P, and Chult DS (2008). Exploring network structure, dynamics, and function using NetworkX. In Proceedings of the 7th Python in Science Conference, Varoquax G, Vaught T, and Millman J, eds., pp. 11–15.

Hayashi H, Nakagami H, Takeichi M, Shimamura M, Koibuchi N, Oiki E, Sato N, Koriyama H, Mori M, Gerardo Araujo R, et al. (2012). HIG1, a novel regulator of mitochondrial γ-secretase, maintains normal mitochondrial function. FASEB J. 26, 2306–2317. [PubMed: 22355194]

Hayashi T, Asano Y, Shintani Y, Aoyama H, Kioka H, Tsukamoto O, Hikita M, Shinzawa-Itoh K, Takafuji K, Higo S, et al. (2015). Higd1a is a positive regulator of cytochrome c oxidase. Proc. Natl. Acad. Sci. USA 112, 1553–1558. [PubMed: 25605899]

Hendrickson RC, Lee AYH, Song Q, Liaw A, Wiener M, Paweletz CP, Seeburger JL, Li J, Meng F, Deyanova EG, et al. (2015). High Resolution Discovery Proteomics Reveals Candidate Disease Progression Markers of Alzheimer's Disease in Human Cerebrospinal Fluid. PLoS ONE 10, e0135365. [PubMed: 26270474]

Hooff GP, Wood WG, Müller WE, and Eckert GP (2010). Isoprenoids, small GTPases and Alzheimer's disease. Biochim. Biophys. Acta 1801, 896–905. [PubMed: 20382260]

Hyman BT, Phelps CH, Beach TG, Bigio EH, Cairns NJ, Carrillo MC, Dickson DW, Duyckaerts C, Frosch MP, Masliah E, et al. (2012). National Institute on Aging-Alzheimer's Association guidelines for the neuropathologic assessment of Alzheimer's disease. Alzheimers Dement. 8, 1–13. [PubMed: 22265587]

Inestrosa NC, and Varela-Nallar L (2014). Wnt signaling in the nervous system and in Alzheimer's disease. J. Mol. Cell Biol. 6, 64–74.

Jahn R, and Scheller RH (2006). SNAREs—engines for membrane fusion. Nat. Rev. Mol. Cell Biol 7, 631–643. [PubMed: 16912714]

Johnson WE, Li C, and Rabinovic A (2007). Adjusting batch effects in microarray expression data using empirical Bayes methods. Biostatistics 8, 118–127. [PubMed: 16632515]

Jones L, Lambert J-C, Wang L-S, Choi S-H, Harold D, Vedernikov A, Escott-Price V, Stone T, Richards A, Bellenguez C, et al.; International Genomics of Alzheimer's Disease Consortium (IGAP) (2015). Convergent genetic and expression data implicate immunity in Alzheimer's disease. Alzheimers Dement. 11, 658–671. [PubMed: 25533204]

Jones JM, Korczak R, Peña RJ, and Braun HJ (2017). CIMMYT Series on Carbohydrates, Wheat, Grains, and Health: Carbohydrates and Vitamins from Grains and Their Relationships to Mild Cognitive Impairment, Alzheimer's Disease, and Parkinson's Disease. Cereal Foods World 62, 65–75.

Juszczak GR, and Stankiewicz AM (2017). Glucocorticoids, genes and brain function. Prog. Neuropsychopharmacol. Biol. Psychiatry

Koizumi H, Fujioka H, Togashi K, Thompson J, Yates JR 3rd, Gleeson JG, and Emoto K (2017). DCLK1 phosphorylates the microtubule-associated protein MAP7D1 to promote axon elongation in cortical neurons. Dev. Neurobiol 77, 493–510. [PubMed: 27503845]

Koldamova R, Schug J, Lefterova M, Cronican AA, Fitz NF, Davenport FA, Carter A, Castranio EL, and Lefterov I (2014). Genome-wide approaches reveal EGR1-controlled regulatory networks associated with neurodegeneration. Neurobiol. Dis 63, 107–114. [PubMed: 24269917]

Langmead B, Trapnell C, Pop M, and Salzberg SL (2009). Ultrafast and memory-efficient alignment of short DNA sequences to the human genome. Genome Biol. 10, R25. [PubMed: 19261174]

Li B, and Dewey CN (2011). RSEM: accurate transcript quantification from RNA-Seq data with or without a reference genome. BMC Bioinformatics 12, 323. [PubMed: 21816040]

Li G, Warden C, Zou Z, Neman J, Krueger JS, Jain A, Jandial R, and Chen M (2013). Altered expression of polycomb group genes in glioblastoma multiforme. PLoS ONE 8, e80970. [PubMed: 24260522]

Li M, Vattulainen S, Aho J, Orcholski M, Rojas V, Yuan K, Helenius M, Taimen P, Myllykangas S, De Jesus Perez V, et al. (2014). Loss of bone morphogenetic protein receptor 2 is associated with abnormal DNA repair in pulmonary arterial hypertension. Am. J. Respir. Cell Mol. Biol 50, 1118–1128. [PubMed: 24433082]

Limon A, Reyes-Ruiz JM, and Miledi R (2012). Loss of functional GABA(A) receptors in the Alzheimer diseased brain. Proc. Natl. Acad. Sci. USA 109, 10071–10076. [PubMed: 22691495]

Lin L, Sun W, Throesch B, Kung F, Decoster JT, Berner CJ, Cheney RE, Rudy B, and Hoffman DA (2013). DPP6 regulation of dendritic morphogenesis impacts hippocampal synaptic development. Nat. Commun 4, 2270. [PubMed: 23912628]

Luchetti S, Bossers K, Van de Bilt S, Agrapart V, Morales RR, Frajese GV, and Swaab DF (2011). Neurosteroid biosynthetic pathways changes in prefrontal cortex in Alzheimer's disease. Neurobiol. Aging 32, 1964–1976. [PubMed: 20045216]

Lunnon K, Keohane A, Pidsley R, Newhouse S, Riddoch-Contreras J, Thubron EB, Devall M, Soininen H, Kłoszewska I, Mecocci P, et al.; AddNeuroMed Consortium (2017). Mitochondrial genes are altered in blood early in Alzheimer's disease. Neurobiol. Aging 53, 36–47. [PubMed: 28208064]

Mandal M, Hamel KM, Maienschein-Cline M, Tanaka A, Teng G, Tuteja JH, Bunker JJ, Bahroos N, Eppig JJ, Schatz DG, and Clark MR (2015). Histone reader BRWD1 targets and restricts recombination to the Igk locus. Nat. Immunol 16, 1094–1103. [PubMed: 26301565]

Manole A, Jaunmuktane Z, Hargreaves I, Ludtmann MHR, Salpietro V, Bello OD, Pope S, Pandraud A, Horga A, Scalco RS, et al. (2017). Clinical, pathological and functional characterization of riboflavin-responsive neuropathy. Brain 140, 2820–2837. [PubMed: 29053833]

Marie SKN, Oba-Shinjo SM, da Silva R, Gimenez M, Nunes Reis G, Tassan J-P, Rosa JC, and Uno M (2016). Stathmin involvement in the maternal embryonic leucine zipper kinase pathway in glioblastoma. Proteome Sci. 14, 6. [PubMed: 26973435]

Marsh SE, Abud EM, Lakatos A, Karimzadeh A, Yeung ST, Davtyan H, Fote GM, Lau L, Weinger JG, Lane TE, et al. (2016). The adaptive immune system restrains Alzheimer's disease pathogenesis

by modulating microglial function. Proc. Natl. Acad. Sci. USA 113, E1316–E1325. [PubMed: 26884167]

Martinez-Mir A, González-Pérez A, Gayán J, Antúnez C, MarÍn J, Boada M, López-Arrieta J, Fernández E, RamÍrez-Lorca R, Saez M, et al. (2013). Genetic Study of Neurexin and Neuroligin Genes in Alzheimer's Disease. J. Alzheimers Dis. 35, 403–412. [PubMed: 23403532]

Massagué J (2012). TGFβ signalling in context. Nat. Rev. Mol. Cell Biol 13, 616–630. [PubMed: 22992590]

Matcovitch-Natan O, Winter DR, Giladi A, Vargas Aguilar S, Spinrad A, Sarrazin S, Ben-Yehuda H, David E, Zelada González F, Perrin P, et al. (2016). Microglia development follows a stepwise program to regulate brain homeostasis. Science 353, aad8670. [PubMed: 27338705]

Mitra K, Carvunis A-R, Ramesh SK, and Ideker T (2013). Integrative approaches for finding modular structure in biological networks. Nat. Rev. Genet 14, 719–732. [PubMed: 24045689]

Mjelle R, Hegre SA, Aas PA, Slupphaug G, Drabløs F, Saetrom P, and Krokan HE (2015). Cell cycle regulation of human DNA repair and chromatin remodeling genes. DNA Repair (Amst.) 30, 53–67. [PubMed: 25881042]

Mostafavi S, Gaiteri C, Sullivan SE, White CC, Tasaki S, Xu J, Taga M, Klein H-U, Patrick E, Komashko V, et al. (2018). A molecular network of the aging human brain provides insights into the pathology and cognitive decline of Alzheimer's disease. Nat. Neurosci 21, 811–819. [PubMed: 29802388]

Poirier R, Cheval H, Mailhes C, Garel S, Charnay P, Davis S, and Laroche S (2008). Distinct functions of egr gene family members in cognitive processes. Front. Neurosci 2, 47–55. [PubMed: 18982106]

R Core Team (2013). R: A language and environment for statistical computing (R Foundation for Statistical Computing).

Recabarren D, and Alarcón M (2017). Gene networks in neurodegenerative disorders. Life Sci. 183, 83–97. [PubMed: 28623007]

Rissman RA, Lee K-F, Vale W, and Sawchenko PE (2007). Corticotropin-releasing factor receptors differentially regulate stress-induced tau phosphorylation. J. Neurosci 27, 6552–6562. [PubMed: 17567816]

Ritchie ME, Phipson B, Wu D, Hu Y, Law CW, Shi W, and Smyth GK (2015). limma powers differential expression analyses for RNA-sequencing and microarray studies. Nucleic Acids Res. 43, e47. [PubMed: 25605792]

Rosenthal SB, Len J, Webster M, Gary A, Birmingham A, and Fisch KM (2018). Interactive network visualization in Jupyter notebooks: visJS2jupyter. Bioinformatics 34, 126–128. [PubMed: 28968701]

Sannerud R, Declerck I, Peric A, Raemaekers T, Menendez G, Zhou L, Veerle B, Coen K, Munck S, De Strooper B, et al. (2011). ADP ribosylation factor 6 (ARF6) controls amyloid precursor protein (APP) processing by mediating the endosomal sorting of BACE1. Proc. Natl. Acad. Sci. USA 108, E559–E568. [PubMed: 21825135]

Schmidt-Edelkraut U, Hoffmann A, Daniel G, and Spengler D (2013). Zac1 regulates astroglial differentiation of neural stem cells through Socs3. Stem Cells 31, 1621–1632. [PubMed: 23630160]

Schneider CA, Rasband WS, and Eliceiri KW (2012). NIH Image to ImageJ: 25 years of image analysis. Nat. Methods 9, 671–675. [PubMed: 22930834]

Settembre C, Di Malta C, Polito VA, Garcia Arencibia M, Vetrini F, Erdin S, Erdin SU, Huynh T, Medina D, Colella P, et al. (2011). TFEB links autophagy to lysosomal biogenesis. Science 332, 1429–1433. [PubMed: 21617040]

Shannon P, Markiel A, Ozier O, Baliga NS, Wang JT, Ramage D, Amin N, Schwikowski B, and Ideker T (2003). Cytoscape: a software environment for integrated models of biomolecular interaction networks. Genome Res. 13, 2498–2504. [PubMed: 14597658]

Sheng M, Sabatini BL, and Südhof TC (2012). Synapses and Alzheimer's disease. Cold Spring Harb. Perspect. Biol. 4, a005777. [PubMed: 22491782]

Silva DF, Selfridge JE, Lu J, e, L., Roy N, Hutfles L, Burns JM, Michaelis EK, Yan S, Cardoso SM, and Swerdlow RH (2013). Bioenergetic flux, mitochondrial mass and mitochondrial morphology

dynamics in AD and MCI cybrid cell lines. Hum. Mol. Genet 22, 3931–3946. [PubMed: 23740939]

Sjölander A, Minthon L, Nuytinck L, Vanmechelen E, Blennow K, and Nilsson S (2013). Functional mannose-binding lectin haplotype variants are associated with Alzheimer's disease. J. Alzheimers Dis 35, 121–127. [PubMed: 23348713]

Strachan GD, Ostrow LA, and Jordan-Sciutto KL (2005). Expression of the fetal Alz-50 clone 1 protein induces apoptotic cell death. Biochem. Biophys. Res. Commun 336, 490–495. [PubMed: 16137655]

Subramanian A, Tamayo P, Mootha VK, Mukherjee S, Ebert BL, Gillette MA, Paulovich A, Pomeroy SL, Golub TR, Lander ES, and Mesirov JP (2005). Gene set enrichment analysis: a knowledge-based approach for interpreting genome-wide expression profiles. Proc. Natl. Acad. Sci. USA 102, 15545–15550. [PubMed: 16199517]

Tan L, Yu JT, Tan MS, Liu QY, Wang HF, Zhang W, Jiang T, and Tan L (2014). Genome-wide serum microRNA expression profiling identifies serum biomarkers for Alzheimer's disease. J. Alzheimers Dis 40, 1017–1027. [PubMed: 24577456]

Thundyil J, Pavlovski D, Sobey CG, and Arumugam TV (2012). Adiponectin receptor signalling in the brain. Br. J. Pharmacol 165, 313–327. [PubMed: 21718299]

Tramutola A, Lanzillotta C, Perluigi M, and Butterfield DA (2017). Oxidative stress, protein modification and Alzheimer disease. Brain Res. Bull 133, 88–96. [PubMed: 27316747]

van Laarhoven T, and Marchiori E (2012). Robust Community Detection Methods with Resolution Parameter for Complex Detection in Protein Protein Interaction Networks. In Proceedings of the 7th IAPR International Conference on Pattern Recognition in Bioinformatics, Shibuya T, Kashima H, Sese J, and Ahmad S, eds., pp. 1–13.

von Bernhardi R, Cornejo F, Parada GE, and EugenÍn J (2015). Role of TGFβ signaling in the pathogenesis of Alzheimer's disease. Front. Cell. Neurosci 9, 426. [PubMed: 26578886]

Wang X-X, Tan M-S, Yu J-T, and Tan L (2014). Matrix Metalloproteinases and Their Multiple Roles in Alzheimer's Disease. BioMed Res. Int 2014, 908636. [PubMed: 25050378]

Wang J, Vasaikar S, Shi Z, Greer M, and Zhang B (2017). WebGestalt 2017: a more comprehensive, powerful, flexible and interactive gene set enrichment analysis toolkit. Nucleic Acids Res. 45 (W1), W130–W137. [PubMed: 28472511]

Watabe-Rudolph M, Song Z, Lausser L, Schnack C, Begus-Nahrmann Y, Scheithauer MO, Rettinger G, Otto M, Tumani H, Thal DR, et al. (2012). Chitinase enzyme activity in CSF is a powerful biomarker of Alzheimer disease. Neurology 78, 569–577. [PubMed: 22323746]

Weeraratna AT, Kalehua A, Deleon I, Bertak D, Maher G, Wade MS, Lustig A, Becker KG, Wood W 3rd, Walker DG, et al. (2007). Alterations in immunological and neurological gene expression patterns in Alzheimer's disease tissues. Exp. Cell Res 313, 450–461. [PubMed: 17188679]

Weissman L, Jo D-G, Sørensen MM, de Souza-Pinto NC, Markesbery WR, Mattson MP, and Bohr VA (2007). Defective DNA base excision repair in brain from individuals with Alzheimer's disease and amnestic mild cognitive impairment. Nucleic Acids Res. 35, 5545–5555. [PubMed: 17704129]

White CC, Yang H-S, Yu L, Chibnik LB, Dawe RJ, Yang J, Klein H-U, Felsky D, Ramos-Miguel A, Arfanakis K, et al. (2017). Identification of genes associated with dissociation of cognitive performance and neuropathological burden: Multistep analysis of genetic, epigenetic, and transcriptional data. PLoS Med. 14, e1002287. [PubMed: 28441426]

Woody SK, Zhou H, Ibrahimi S, Dong Y, and Zhao L (2016). Human ApoE ε2 Promotes Regulatory Mechanisms of Bioenergetic and Synaptic Function in Female Brain: A Focus on V-type H+-ATPase. J. Alzheimers Dis 53, 1015–1031. [PubMed: 27340853]

Yu G, Wang L-G, Han Y, and He Q-Y (2012). clusterProfiler: an R package for comparing biological themes among gene clusters. OMICS 16, 284–287. [PubMed: 22455463]

Yung YC, Stoddard NC, Mirendil H, and Chun J (2015). Lysophosphatidic Acid signaling in the nervous system. Neuron 85, 669–682. [PubMed: 25695267]

Zhang B, Gaiteri C, Bodea L-G, Wang Z, McElwee J, Podtelezhnikov AA, Zhang C, Xie T, Tran L, Dobrin R, et al. (2013). Integrated systems approach identifies genetic nodes and networks in late-onset Alzheimer's disease. Cell 153, 707–720. [PubMed: 23622250]

Zhang C, Kuo C-C, Moghadam SH, Monte L, Campbell SN, Rice KC, Sawchenko PE, Masliah E, and Rissman RA (2016). Corticotropin-releasing factor receptor-1 antagonism mitigates beta amyloid pathology and cognitive and synaptic deficits in a mouse model of Alzheimer's disease. Alzheimers Dement. 12, 527–537. [PubMed: 26555315]

Zhu Q-B, Unmehopa U, Bossers K, Hu Y-T, Verwer R, Balesar R, Zhao J, Bao A-M, and Swaab D (2016). MicroRNA-132 and early growth response-1 in nucleus basalis of Meynert during the course of Alzheimer's disease. Brain 139, 908–921. [PubMed: 26792551]

Highlights

- RNA expression profiling of 414 Alzheimer's disease and non-demented controls
- Integration of transcriptomic profiles with brain tissue-specific protein interactome
- Revealed biologically distinct clusters by Louvain algorithm for community detection
- Characterized transcriptional regulators across all clusters

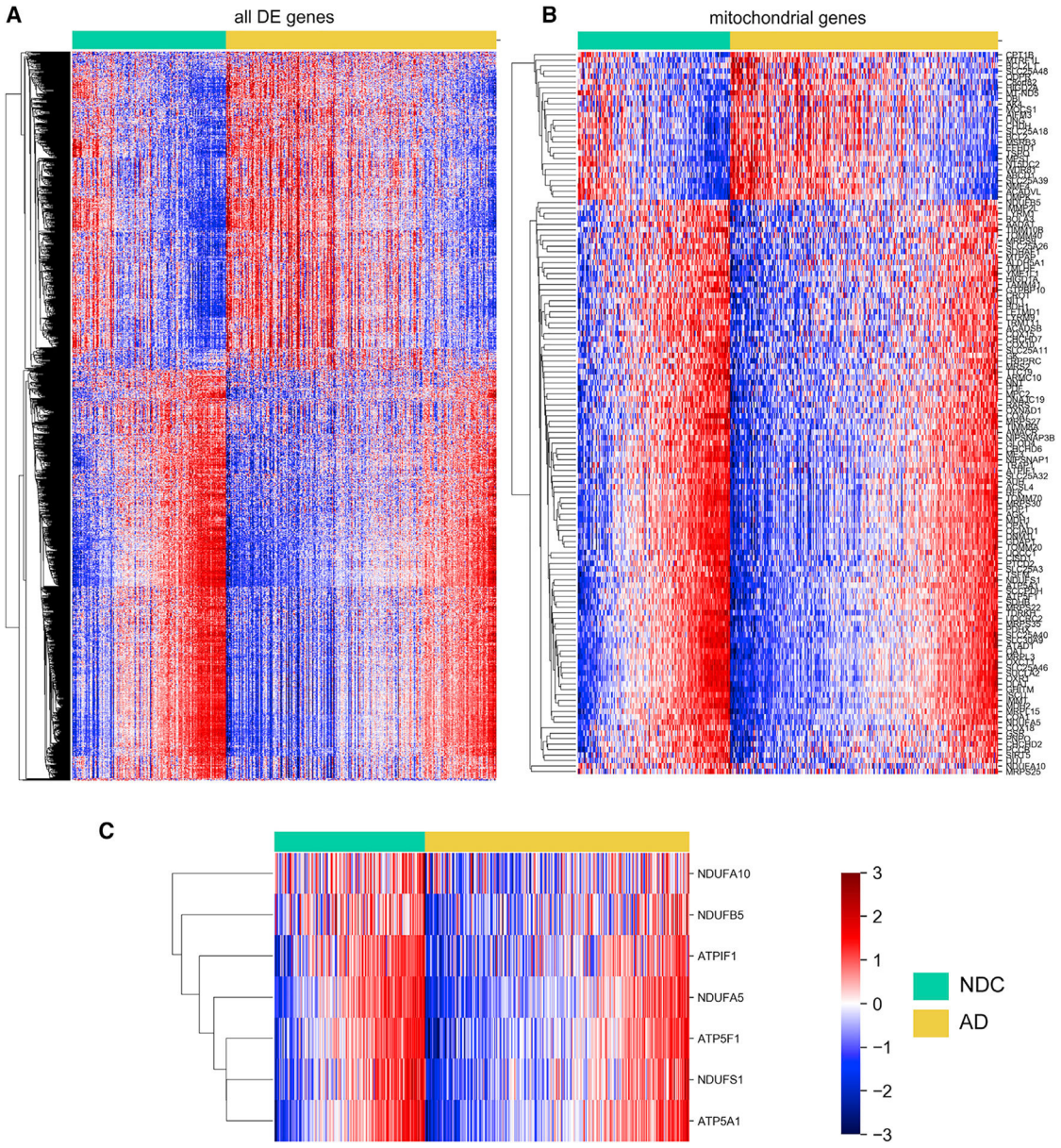

Figure 1. Global Gene Expression Patterns Highlight Differences in Alzheimer's Disease (AD) Relative to Non-demented Controls (NDCs)

(A) Heatmap of all differential expressed genes (N = 1,722) clustered by phenotype In the prefrontal cortex.

(B) Most differentially expressed mitochondrial genes are downregulated In AD, but a small proportion are upregulated relative to NDCs.

(C) Nuclear encoded oxidative phosphorylation (OXPHOS) genes are dysregulated in AD.

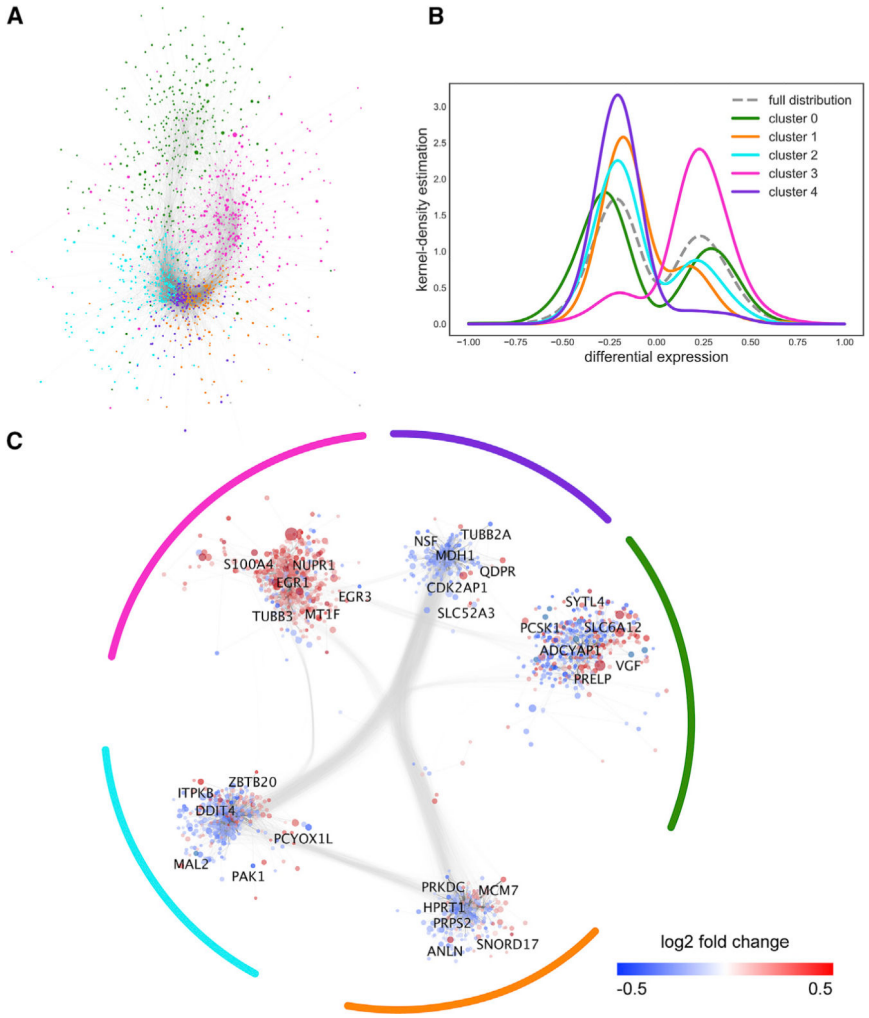

Figure 2. Composite Gene-Protein Interaction Network Reveals Significant Clustering in AD

(A) AD subnetwork with cluster ID mapped to node color. The subnetwork is composed of genes differentially expressed in AD compared with NDCs and overlaid onto the GIANT brain-specific interactome. Node positions are fully determined from the spring layout. Clusters are determined using the Louvain modularity maximization algorithm.

(B) Distributions of log fold change values in each cluster, as well as in the entire AD subnetwork. Distribution curves were determined using a kernel-density estimation function (see also Figure S1).

(C) AD subnetwork with node positions biased by cluster membership. Node colors are mapped to the log fold change between AD and NDC. Node size represents the significance (FDR) of the gene's differential expression in AD compared with NDC.

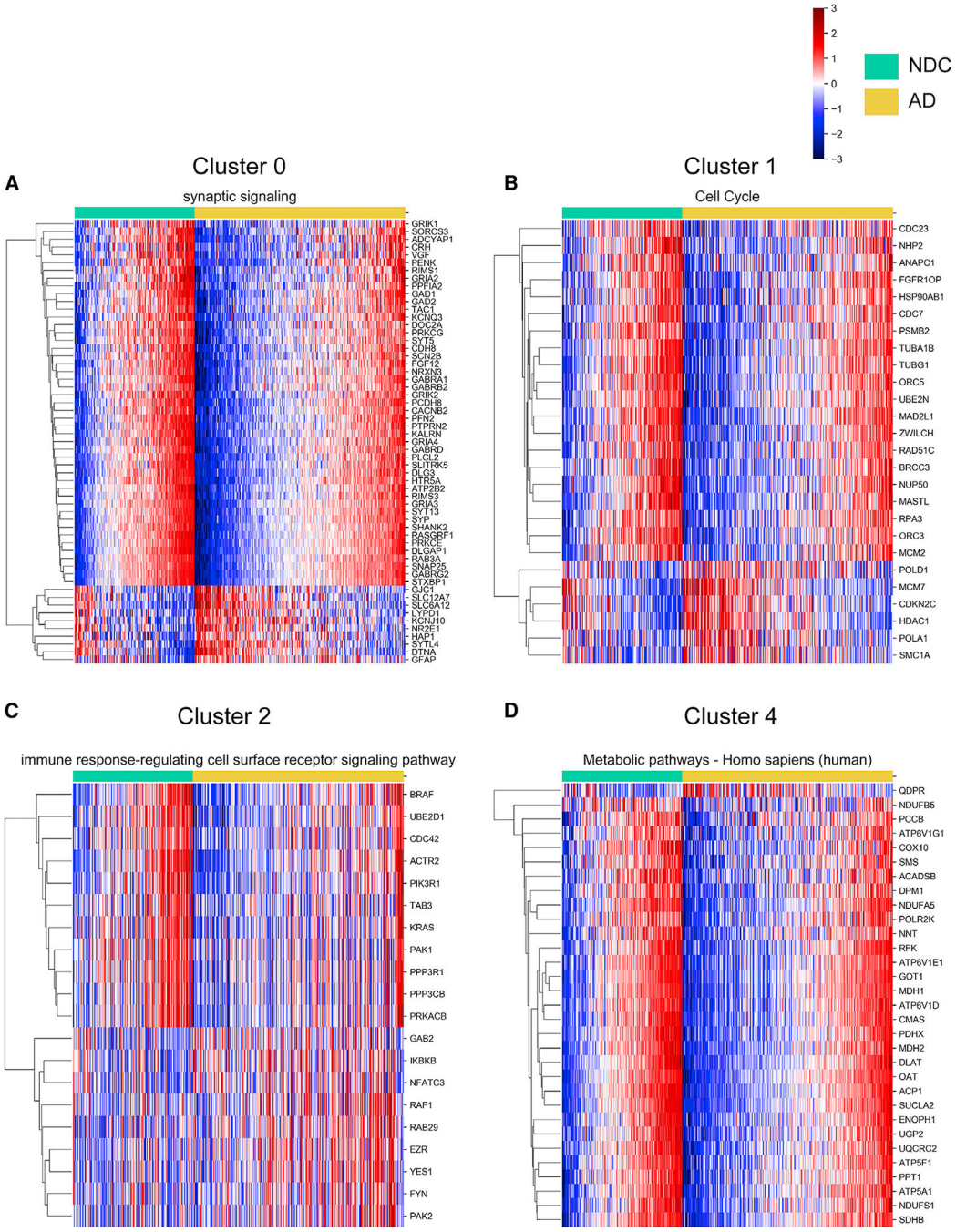

Figure 3. Heatmaps of Top Enriched Pathways from Each Functionally Distinct Cluster

(A–D) Enriched pathways correspond to (A) neurotransmitter-related signaling in cluster 0, (B) DNA repair and cell-cycle control in cluster 1, (C) immune response in cluster 2, and (D) metabolism and bioenergetics in cluster 4. No enriched pathways were identified for cluster 3 (see also Figures S2–S6).

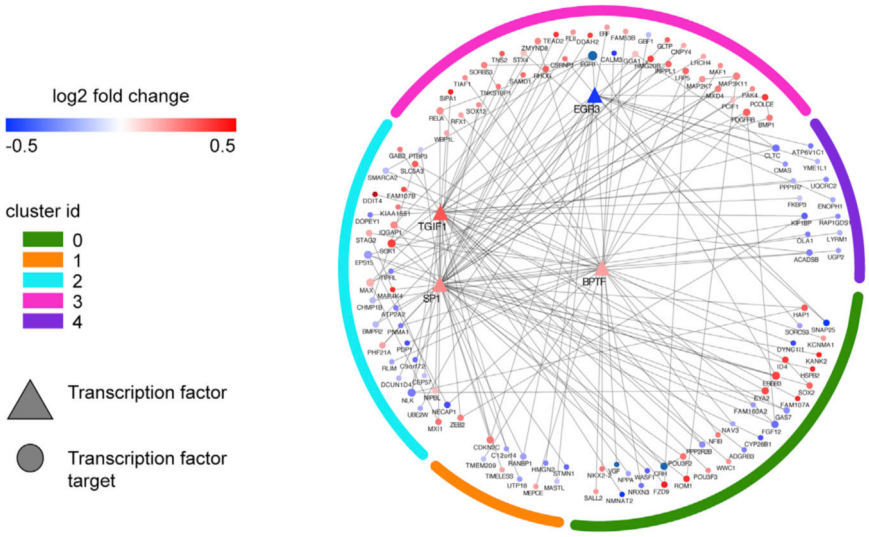

Figure 4. Transcriptional Regulatory Network in AD

Four candidate transcription factors (TFs) identified in AD, along with all differentially expressed targets in the AD subnetwork, are displayed in a circular layout, ordered by cluster membership. TFs are displayed inside the circle as triangles. The log fold change between AD and NDC is mapped to the node color. *BPTF* does not belong to any cluster. The TF subnetwork highlights the connections between TFs and targets, along with connections between targets (see also Figure S7).

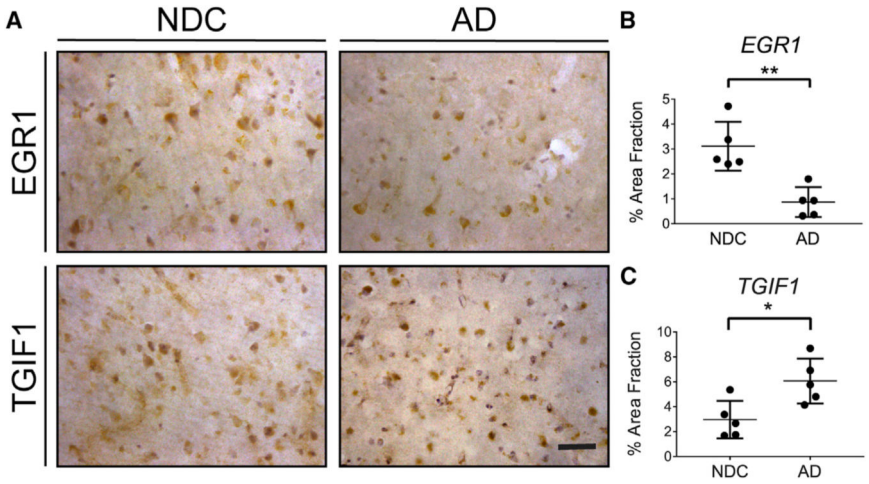

Figure 5. Protein Expression of TGIF and EGR1 in Human Prefrontal Cortex Tissue Samples

(A) Representative images of prefrontal cortex from NDCs and AD brains immunohistochemically stained for *TGIF1* and *EGR1,* which is a direct target of *EGR3.*

(B and C) Bar graphs of relative area fraction for (B) *EGR1*-stained cells and (C) *TGIF1*-stained cells are consistent with the RNA-level expression changes.

Data are represented as mean ± SD for n = 5 per group. Each tissue section contributed to an average of 20 image fields. Scale bar is 50 μm. *p < 0.05, **p < 0.01.

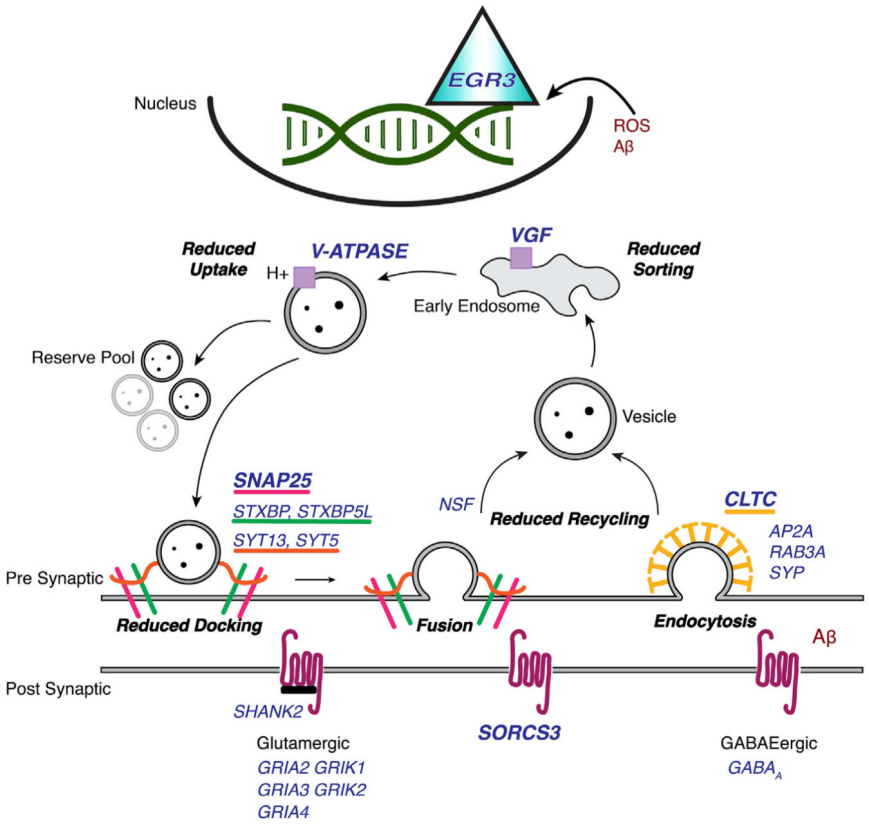

Figure 6. Loss of EGR3 Regulation Mediates Synaptic Deficits by Targeting the Synaptic Vesicle Cycle

Genes names in blue imply downregulation in AD relative to NDCs, and direct targets of *EGR3* are shown in bold. Reduced proton gradient (*V-ATPASE*) results in inefficient neurotransmitter uptake. Downregulation of key essential proteins, including *SNAP25,* imply reduced vesicle docking at the presynaptic membrane. Inefficient disassociation of actively fused vesicles, along with reduced clathrin (*CLTC*), leads to decreased vesicle recycling. This creates a negative feedback loop and, after multiple cycles, leads to eventual depletion in reserve vesicles. Downregulation of *EGR3* results in reduced content and number of vesicle fusion activities, priming the cells toward ineffective synaptic transmission.

Table 1.

Sample Demographics of the Subjects Included in the Study

	NDCs	AD
Demographic Variable	**(N = 151)**	**(N = 263)**
Female sex, No. (%)	92 (60.9)	185 (70.3)
Education, years	16.5 (3.6)	16.2 (3.5)
MMSE	28.6 (1.0)	14.5 (7.5)
APOE ε4, No. (%)	20 (13.2)	90 (34.2)
Age at death, years	85.2 (6.6)	90.9 (5.9)
PMI, h	7.4 (4.4)	7.6 (5.2)
RIN	7.2 (1.0)	6.9 (0.9)

APOE, apolipoprotein E; MMSE, Mini-Mental State Examination; PMI, postmortem interval; RIN, RNA integrity number; NDCs; non-demented controls; AD, Alzheimer's disease. Data are presented as mean (SD) unless specified.

KEY RESOURCES TABLE

REAGENT or RESOURCE	SOURCE	IDENTIFIER
Antibodies		
Mouse polyclonal anti-IgG	Vector Laboratories	Cat# BA-2000; RRID: AB_2313581
Mouse monoclonal anti-TGIF(H-1)	Santa Cruz Biotechnology	Cat# sc-17800; RRID: AB_2202719
Rabbit monoclonal anti-EGR1	Cell Signaling Technology	Cat# 4153; RRID: AB_2097038
Biological Samples		
Human BA9 brain tissue blocks	University of California San Diego Shiley-Marcos Alzheimer's Disease Research Center Brain Bank	http://adrc.ucsd.edu/neuropath.html
Chemicals, Peptides, and Recombinant Proteins		
Normal Horse Serum	Vector Laboratories	Cat# S-2000; RRID: AB_2336617
Critical Commercial Assays		
DAB Substrate Kit (3,3′-diaminobenzidine)	Vector Laboratories	Cat# SK-4100; RRID: AB_2336382
VECTASTAIN Elite ABC-Peroxidase Kit	Vector Laboratories	Cat# PK-6100; RRID: AB_2336819
Deposited Data		
RNaseq	Synapse	https://www.synapse.org/#!Synapse:syn3388564
Clinical_Data	Synapse	https://www.synapse.org/#!Synapse:syn3157322
Software and Algorithms		
visJS2jupyter v0.1.16	Rosenthal et al., 2018	https://pypi.org/project/visJS2jupyter/
Cytoscape v3.6.1	Shannon et al., 2003	https://cytoscape.org/
NetworkX v1.11	Hagberg et al., 2008	https://networkx.github.io/documentation/networkx-1.11/
Python v2.7	N/A	https://www.python.org/download/releases/2.7/
Webgestalt 2017	Wang et al., 2017	http://www.webgestalt.org/2017/option.php
gseapy v0.8.4	N/A	https://pypi.org/project/gseapy/
COMBAT v3.20.0	Johnson et al., 2007	https://bioconductor.org/packages/release/bioc/html/sva.html
limma v3.38.3	Ritchie et al., 2015	https://bioconductor.org/packages/release/bioc/html/limma.html
seaborn v0.9.0	N/A	https://seaborn.pydata.org/
R v3.5.1	R Core Team, 2013	http://www.R-project.org/
ImageJ	Schneider et al., 2012	https://imagej.nih.gov/ij/
GraphPad Prism 7	GraphPad Software Inc	http://www.graphpad.com
Other		
Leica DM5500 B microscope	Leica Microsystems	N/A